Synthesis and Micellization of Coil−Rod−Coil Ruthenium(II) Terpyridine Assemblies

Manuela Chiper,[†,‡] Andreas Winter,[†,‡] Richard Hoogenboom,[†,‡] Daniel A. M. Egbe,[†,‡] Daan Wouters,[†,‡] Stephanie Hoeppener,[†,‡] Charles-Andre Fustin,[§] Jean-Francois Gohy,[§] and Ulrich S. Schubert*[,†,‡,∥]

Laboratory of Macromolecular Chemistry and Nanoscience, Eindhoven University of Technology, 5600 MB Eindhoven, The Netherlands; Dutch Polymer Institute (DPI), P.O. Box 513, 5600 MB Eindhoven, The Netherlands; Unité CMAT, Université catholique de Louvain, Place L. Pasteur 1, 1348 Louvain-la-Neuve, Belgium and Laboratory of Organic and Macromolecular Chemistry, Friedrich-Schiller-Universität Jena, Humboldtstr. 10, D-07743 Jena, Germany

Received May 31, 2008; Revised Manuscript Received September 26, 2008

ABSTRACT: Four different coil−rod−coil metallo-supramolecular amphiphilic copolymers have been synthesized via Ru(II) terpyridine complexation, using monoterpyridine end-functionalized poly(ethylene glycol) as hydrophilic block **A** and different rigid-rod conjugated ditopic terpyridyl ligands as hydrophobic segment **B**. Those structures are reminiscent of **ABA** triblock copolymers. Herein, we report for the first time the synthesis and characterization as well as the photophysical and electrochemical properties of these novel Ru(II) **ABA** assemblies. The aqueous self-assembly of these synthesized materials was studied by cryo-transmission electron microscopy and dynamic light scattering, demonstrating a significant influence of the various middle segments **B** on the size of the obtained micelles.

Introduction

Supramolecular materials can be constructed via weak and reversible noncovalent interactions such as hydrogen bonding, metal coordination, $\pi-\pi$ or host−guest interactions, electrostatic effects, and solvophobic or van der Waals forces.[1] The possibility of combining various functional ligands with a large range of transition metal ions has made metal−ligand coordination an important method in the field of supramolecular chemistry.[2−34] Metal−ligand interactions vary from very strong to very weak according to the combination of metal ion and ligand used. Most of these supramolecular "connections" are weaker than covalent bonds making them more labile and dynamical, providing the possibility of forming "switchable" systems under certain conditions (e.g., following an external trigger).[5−8] The architecture of supramolecular metal-containing polymers can be controlled by the geometry of the bridging ligands that influences the coordination of metal ions.[9−13] One of the most promising chelating ligands in this area is certainly 2,2′:6′,2″-terpyridine. The extraordinary binding affinity toward most transition metal ions due to $d\pi \rightarrow p\pi^*$ bonding, together with the strong chelating effect, makes terpyridines appealing building blocks for the design and the construction of supramolecular assemblies.[4,14−17] From the large range of transition metal ions, ruthenium(II) represents one of the most favorable ions in the engineering of robust terpyridine coordination assemblies because it allows the direct synthesis of both heteroleptic as well as homoleptic systems.[18] In addition, ruthenium terpyridine complexes possess interesting photophysical and electrochemical properties, which are strongly influenced by the electronic characteristics of the lateral substituents.[19−22] Rigid-rod-like ditopic terpyridyl ligands have been used as precursors for polymetallic architectures,[23−25] which can be applied for the preparation of luminescent or electrochemical sensors.[26−30] A variety of other examples of terpyridine-containing metallo-supramolecular polymers can be found in the literature.[9,31−34] Because of the stiff structural design of the spacer, rigid-rod-like ditopic terpyridyl ligands are successfully leading to the formation of linear supramolecular metal-containing structures.[35−37] Furthermore, the addition of side chains on the rigid spacer of the ditopic terpyridyl ligands can significantly improve the solubility in organic solvents of the substituted systems in comparison to the poorly soluble unsubstituted analogous compounds.[22,30,38] This type of conjugated rigid-rod-like ditopic ligands can also be considered as promising candidates for the synthesis of block copolymers based on ruthenium(II) terpyridine complexes, which are susceptible to self-assemble into nanostructured materials (e.g., micelles in a selective solvent) when incompatible blocks are chosen.

In the present contribution we focus on the synthesis and characterization of novel coil−rod−coil macromolecular architectures based on ruthenium(II) terpyridine complexes that resemble **ABA** triblock copolymers. Several examples of **AB**, **ABA**, or **ABC** block copolymers based on Ru(II) bis(terpyridine) connectivities were already described in the literature.[39−42] These types of metallo-supramolecular block copolymers have proven to be attractive precursors for complex self-assembled structures.[43,44] In this work, **A** is a monoterpyridine end-functionalized poly(ethylene glycol), a water-soluble random coil polymer, and **B** is a rigid conjugated segment end-capped at both ends by terpyridyl ligands. For the preparation of the hydrophobic segments **4a**−**d**, terpyridine units were introduced into both ends of rigid conjugated chains via several routes, as reported previously.[22] The resulting ligands **4a**−**d** were assembled into **ABA** supramolecular structures **5a**−**d** via Ru(II) complexation of monoterpyridine poly(ethylene glycol) **1**. Besides the synthesis and characterization, the aqueous micellization of those coil−rod−coil amphiphilic **ABA** triblock assemblies is described and studied by cryo-transmission electron microscopy and dynamic light scattering.

* Corresponding author. Fax: (+31) (0)40 2474186. E-mail: u.s.schubert@tue.nl.
† Eindhoven University of Technology.
‡ Dutch Polymer Institute.
§ Université catholique de Louvain.
∥ Friedrich-Schiller-Universität Jena.

10.1021/ma801217v CCC: $40.75
Published on Web 10/30/2008

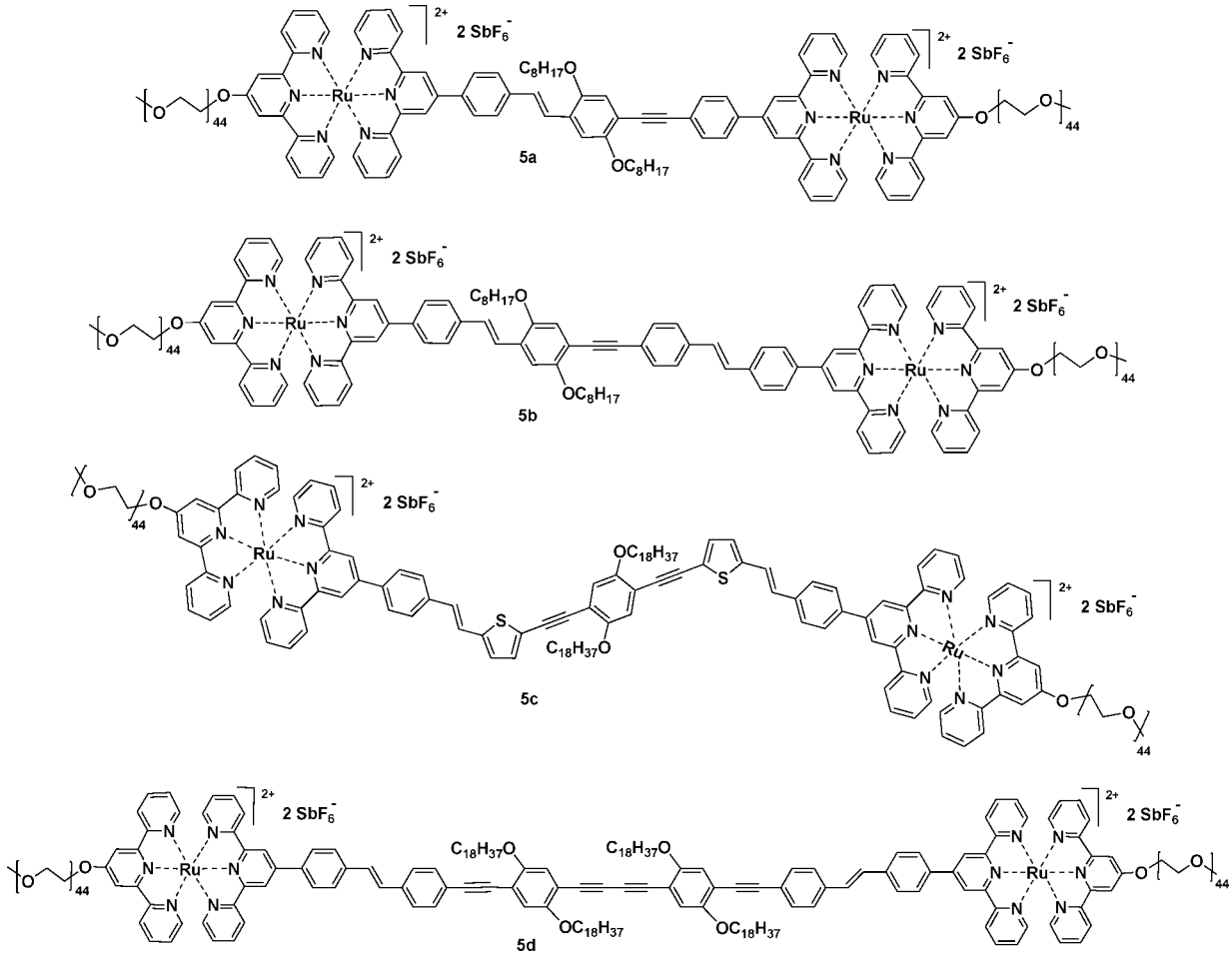

Figure 1. Schematic representation of the chemical structures of the synthesized **ABA** triblock assemblies **5a−d**.

Scheme 1. Schematic Representation of the Synthesis of Monocomplex Macroligand 2, Model Complex 3, and ABA Triblock Assemblies 5a−d

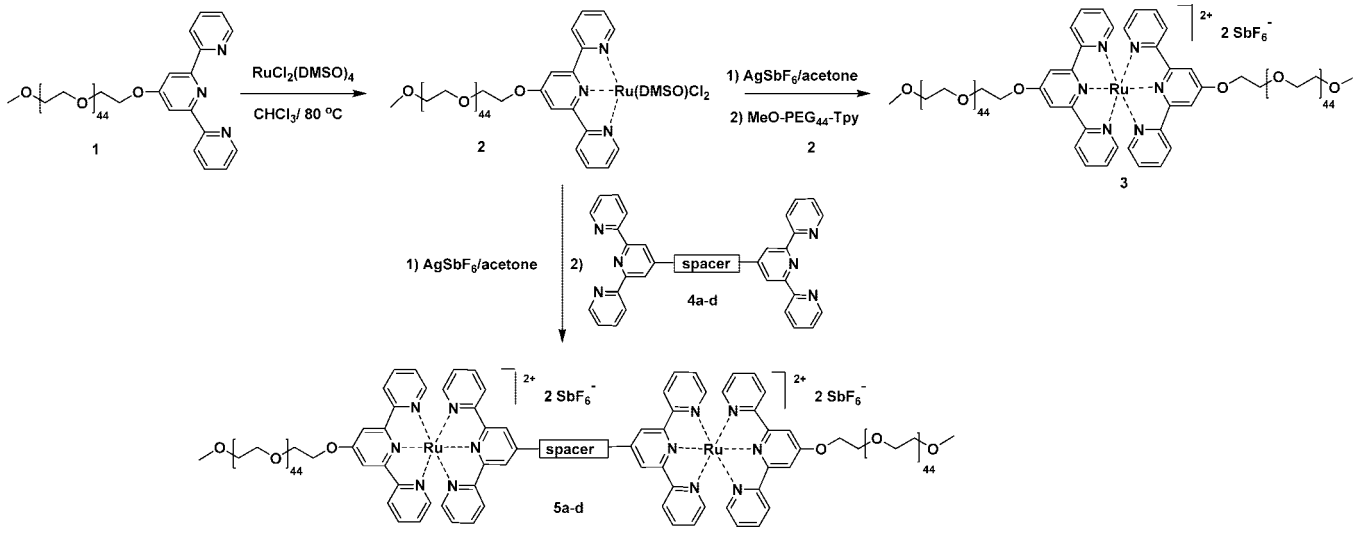

Experimental Section

Materials and General Experimental Details. All chemicals were of reagent grade and used as received unless otherwise specified. $AgSbF_6$ was purchased from Aldrich. $Ru(DMSO)Cl_2$ was prepared according to literature procedures.[45] The preparation and full characterization of the ditopic terpyridine ligands **4a−d** is described elsewhere.[22] Preparative size exclusion chromatography was performed on BioBeads S-X1 columns using dichloromethane or tetrahydrofuran as eluents.

Instrumentation. Size exclusion chromatograms were measured on a Waters SEC system consisting of an isocratic pump, a solvent degasser, a column oven, a 2996 photodiode array (PDA) detector, a 2414 refractive index detector, a 717 plus autosampler, and a Waters Styragel HT 4 GPC column (with 10 μm particles) with a precolumn installed. The eluent was *N,N*-dimethylformamide (DMF) containing 5 mM NH_4PF_6 as additive at a flow speed of 0.5 mL/min. Narrowly distributed linear poly(ethylene glycol) standards with a M_w range from 970 to 40 000 Da were used for

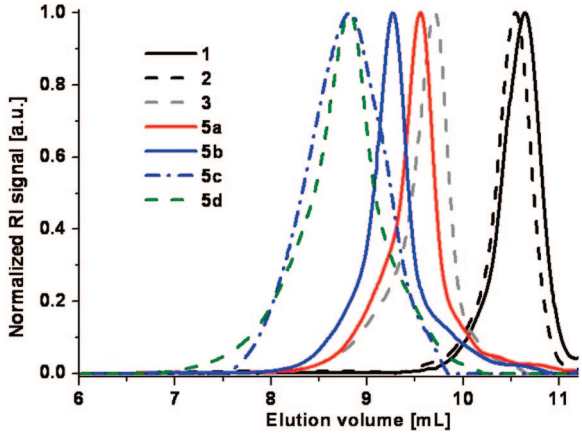

Figure 2. SEC elution curves (RI detector) for monoterpyridine-PEG **1**, monocomplex macroligand **2**, model complex **3**, and **ABA** triblock assemblies **5a**−**d**.

the calibration to calculate M_n and PDI. The column temperature was 50 °C. Nuclear magnetic resonance spectra were recorded on a Varian Gemini 400 MHz spectrometer at 298 K. Chemical shifts are reported in parts per million (δ) downfield from an internal standard, tetramethylsilane (TMS) in CD_2Cl_2. UV−vis spectra were recorded on a Perkin-Elmer Lamda-45 (1 cm cuvettes, $CHCl_3$ or CH_3CN). Emission spectra were recorded on a Perkin-Elmer LS50B luminescence spectrometer (1 cm cuvettes, CH_3CN). Electrochemical experiments were performed using an Autolab PGSTAT30 model potentiostat. A standard three-electrode configuration was used, with a platinum-disk working electrode, a platinum-rod auxiliary electrode, and Ag/AgCl reference electrode. Ferrocene was added at the end of each experiment as an internal standard. The oxidation potentials are quoted versus the ferrocene/ferrocenium couple (Fc/Fc^+). The solvent used was CH_2Cl_2 (freshly distilled from CaH_2), containing 0.1 M n-Bu_4PF_6. The scan rate was 100 mV/s.

Dynamic light scattering (DLS) experiments were performed on a Malvern CGS-3 equipped with a He−Ne laser (633 nm, 22 mW) and an ALV-5000/EPP correlator. The measurements have been performed at an angle of 90° and at a temperature of 25 °C. The results were analyzed by the CONTIN method which is based on an inverse-Laplace transformation of the data and which gives access to a size distribution histogram for the analyzed micellar solutions. Cryogenic transmission electron microscopy (cryo-TEM) measurements were performed on a FEI Tecnai 20, type Sphera TEM operating at 200 kV (LaB6 filament). Images were recorded with a bottom mounted 1k × 1k Gatan CCD camera. A Gatan cryo-holder operating at −170 °C was used for the cryo-TEM measurements. R2/2 Quantifoil (Jena) grids were purchased from SPI. Cryo-TEM specimens were prepared applying 3 μL aliquots to the grids within the environmental chamber (22 °C, relative humidity 100%) of an automated vitrification robot (FEI Vitrobot Mark III). Excess liquid was blotted away (−2 mm offset, 2.5 s) with filter paper within the environmental chamber of the Vitrobot. The grids were subsequently shot through a shutter into melting ethane placed just outside the environmental chamber. Vitrified specimens were stored under liquid nitrogen before imaging. Prior to blotting, the grids were made hydrophilic by surface plasma treatment using a Cressington 208 carbon coater operating at 5 mA for 40 s.

Synthesis of Macroligand Monocomplex 2. A mixture of $Ru(DMSO)_4Cl_2$ (261 mg, 540 mmol) and α-terpyridine-ω-methylpoly(ethylene glycol), **1** (1000 mg, 450 mmol), in argon-degassed $CHCl_3$ (10 mL) was refluxed overnight. During this time the solution turned brown. After being cooled to ambient temperature, the solution was concentrated in vacuo. The crude product was further purified by preparative size exclusion chromatography (BioBeads SX-1, CH_2Cl_2), followed by precipitation from dichloromethane into diethyl ether. Yield: 80%.^{1}H NMR (400 MHz, CD_2Cl_2, 25 °C): δ = 9.21 (m, 2H, H^6, $H^{6''}$), 8.17 (d, 4H, J = 4 Hz; $H^{3'}$, $H^{5'}$), 7.89 (m, 4H, H^3, $H^{3''}$), 7.74 (s, 4H, J = 4 Hz; H^4, $H^{4''}$), 7.57 (m, 4H, H^5, $H^{5''}$), 4.33 (m, 2H, tpyOCH_2), 3.87 (m, 2H, tpyOCH_2CH_2), 3.77−3.52 (m, 44H, PEG-backbone), 3.24 (s, 3H; OCH_3). UV−vis ($CHCl_3$): λ_{max}: 242, 275, 309, 402, 477. SEC (RI detector; PEG calibration): M_n = 2500 g mol^{-1}; M_w = 2800 g mol^{-1}, PDI = 1.12.

Table 1. Comparison of the Photophysical and Electrochemical Properties of the Bis(terpyridine) Ligands 4a−d and Ru(II) ABA Triblock Assemblies 5a−d

compound	$\lambda_{abs,max}$ [nm][a]	E_g^{opt} [eV][b]	$\lambda_{em,max}$ [nm][a]	Φ_{fl} [%][c]	E^o [V][d]
4a	281, 326, 394	2.72	459	81	
4b	339, 371, 419	2.78	490	68	
4c	280, 424	2.56	487	54	
4d	284, 348, 406	2.72	458	60	
5a	272, 306, 498	2.27	540		1.194
5b	273, 306, 356, 498	2.26	538		1.203
5c	271, 303, 492	2.26	518		1.201
5d	272, 305, 401, 491	2.29	471		1.183

[a] The absorption and emission spectra of **4a**−**d** have been recorded at room temperature in $CHCl_3$.[22] The absorption and emission spectra of **5a**−**d** have been recorded at room temperature in CH_3CN. For all spectra a concentration of 10^{-5} M was used. Photoluminescence spectra were obtained at an excitation wavelength of λ_{ex} = 400 nm. [b] Optical band gaps were estimated from the absorption spectra in solution by extrapolating the tails of the lower energy peaks. [c] Quantum yields were measured using quinine sulfate (Φ_{fl} = 55%) as a reference.[58] [d] All CV spectra were recorded in CH_2Cl_2 (freshly distilled from CaH_2) containing 0.1 M n-Bu_4PF_6 vs Ag/Ag^+ reference electrode. The shown data refers to the oxidation potential Ru(II)/Ru(III).

Synthesis of Model Complex 3. A suspension of α-terpyridine-ω-methylpoly(ethylene glycol)−$RuCl_2$(DMSO) (100 mg, 0.04 mmol), **2**, and $AgSbF_6$ (27.27 mg, 0.08 mmol) was refluxed overnight in acetone, followed by filtration of the formed AgCl. The [α-terpyridine-ω-methylpoly(ethylene glycol) Ru(II)(DMSO)-$(OCMe_2)_2]^{2+}(SbF_6^-)_2$ solution was then added to a solution of the monoterpyridine end-functionalized poly(ethylene glycol) **1** (68.1 mg, 0.03 mmol) in acetone. The reaction mixture was heated under reflux for 48 h. After cooling to ambient temperature, the reaction mixture was filtered through Celite and then purified by preparative size exclusion chromatography (BioBeads SX-1, CH_2Cl_2). Yield: 38%. ^{1}H NMR (400 MHz, CD_2Cl_2, 25 °C): δ = 8.39 (d, 4H, J = 8 Hz; H^3, $H^{3''}$), 8.27 (s, 4H; $H^{3'}$, $H^{5'}$), 7.88 (t, 4H, J = 7.6 Hz, 3.6 Hz; H^4, $H^{4''}$), 7.35 (d, 4H, J = 4 Hz; H^6, $H^{6''}$), 7.19 (t, 4H, J = 6.6 Hz, 3.6 Hz; H^5, $H^{5''}$), 4.73 (m, 4H, tpyOCH_2), 4.12 (m, 4H, tpyOCH_2CH_2), 3.78−3.52 (m, 90 H; PEG backbone), 3.36 (s, 6H; OCH_3). UV−vis ($CHCl_3$): λ_{max}: 267, 305, 486. SEC (RI detector; PEG calibration): M_n = 9400 g mol^{-1}; M_w = 10 000 g mol^{-1}; PDI = 1.05.

General Synthesis of ABA Triblock Assemblies 5a−d. A suspension of α-terpyridine-ω-methylpoly(ethylene glycol)−$RuCl_2$-(DMSO) (0.1 mmol), **2**, and $AgSbF_6$ (0.3 mmol) was refluxed overnight in acetone, followed by filtration of the formed AgCl. The [α-terpyridine-ω-methylpoly(ethylene glycol)Ru(II)(DMSO)-$(OCMe_2)_2]^{2+}(SbF_6^-)_2$ solution was then added to a solution of the ditopic ligand **4a**−**d** (0.03 mmol) in acetone. The reaction mixture was heated under reflux for 48 h. After cooling to ambient temperature, the reaction mixture was filtered through Celite and then purified by preparative size exclusion chromatography (BioBeads SX-1, CH_2Cl_2). Yields: 25%, 50%, 20%, and 39%, respectively.

5a: ^{1}H NMR (400 MHz, CD_2Cl_2, 25 °C): δ = 8.87 (s, 4H), 8.57 (m, 4H), 8.41 (d, 4H, J = 4 Hz), 8.33 (s, 4H), 8.15 (m, 4H), 7.97−7.87 (m, 10H,), 7.76 (d, 2H, J = 4 Hz), 7.69 (d, 2H), 7.43−7.34 (m, 9H), 7.27 (t, 4 H, J = 2 Hz), 7.20 (t, 4H, J = 4 Hz), 7.16 (s, 1H,), 4.75 (m, 4H), 4.19 (m, 2H), 4.11 (m, 6H), 3.84−3.40 (m, 90H), 3.34 (s, 6H), 1.97 (m, 4H), 1.60 (m, 4H), 1.23−1.45 (m, 16H), 0.91 (m, 6H). UV−vis ($CHCl_3$): λ_{max}: 272, 306, 489. SEC (RI detector; PEG calibration): M_n = 11 000 g mol^{-1}; M_w = 11 300 g mol^{-1}; PDI = 1.02.

5b: ^{1}H NMR (400 MHz, CD_2Cl_2, 25 °C): δ = 8.89 (s, 4 H), 8.56 (m, 4 H), 8.41 (m, 4 H), 8.34 (s, 4 H), 8.17 (m, 4 H),

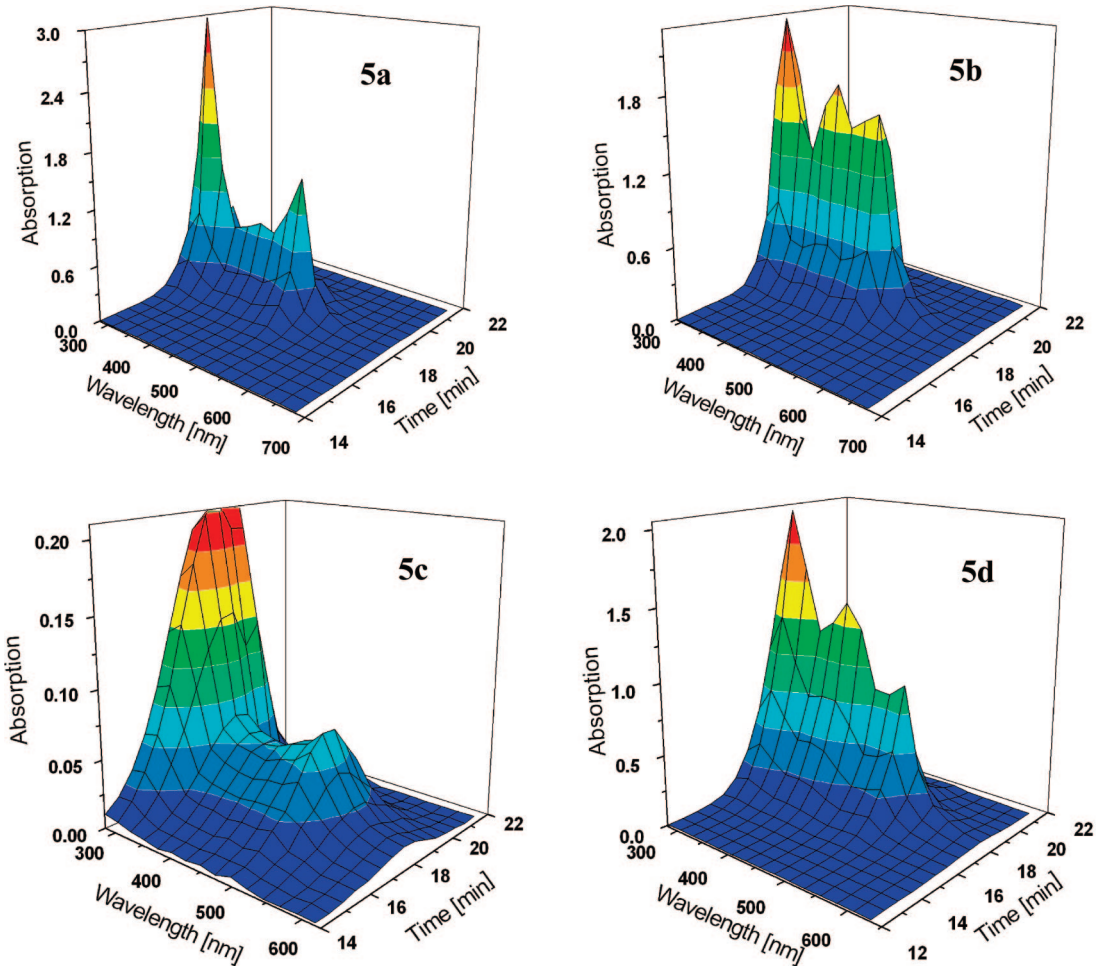

Figure 3. SEC elution curves (photodiode array detector) of the **ABA** triblock assemblies **5a−d**.

7.98−7.90 (m, 10 H), 7.65 (m, 2 H), 7.42 (m, 2 H), 7.37 (m, 2 H), 7.28 (m, 4 H), 7.21 (m, 4 H), 7.16 (s, 1 H), 4.76 (m, 4 H), 4.19 (m, 2 H), 4.11 (m, 6 H), 3.77−3.42 (m, 90 H), 3.34 (s, 6 H), 1.97 (m, 4 H,), 1.66 (m, 4 H), 1.17−1.31 (m, 16 H), 0.85 (m, 6 H). UV−vis ($CHCl_3$): λ_{max}: 273, 306, 356, 498. SEC (RI detector; PEG calibration): M_n = 9700 g mol^{-1}; M_w = 10 700 g mol^{-1}; PDI = 1.10.

5c: ^{1}H NMR (400 MHz, CD_2Cl_2, 25 °C): δ = 8.87 (s, 4H), 8.80 (s, 4 H). 8.74 (m, 4 H), 8.40 (m, 4 H), 7.93 (m, 4 H), 7.89 (m, 4 H), 7.61 (m, 4 H), 7.37 (m, 4 H), 7.29 (m, 2 H), 7.18 (m, 2H), 6.99 (m, 4 H), 4.76 (m, 4H), 4.11 (m, 4 H), 3.91−3.37 (m, 90 H), 3.35 (s, 6 H) 1.65 (m, 4 H), 1.44 (m, 4 H), 1.12−1.35 (m, 56 H), 0.89 (m, 6 H). UV−vis ($CHCl_3$): λ_{max}: 271, 303, 492. SEC (RI detector; PEG calibration): M_n = 11 500 g mol^{-1}; M_w = 13 400 g mol^{-1}; PDI = 1.16.

5d: ^{1}H NMR (400 MHz, CD_2Cl_2, 25 °C): δ = 8.90 (s, 4H), 8.55 (m, 4 H). 8.42 (m, 4 H), 8.34 (s, 4 H), 8.16 (m, 4 H), 7.94 (m, 4 H), 7.89 (m, 4 H), 7.61 (m, 4 H), 7.42 (m, 7 H), 7.39 (m, 2 H), 7.28 (m, 2H) 7.21 (m, 3 H), 7.00 (m, 3 H), 4.76 (m, 4H), 3.66−3.46 (m, 90 H), 3.35 (s, 6 H), 3.84 (m, 8 H), 1.85 (m, 8 H), 1.72 (m, 8 H), 1.59 (m, 8 H), 1.17−1.43 (m, 104 H), 0.87 (m, 12 H). UV−vis ($CHCl_3$): λ_{max}: 272, 303, 401, 491. SEC (RI detector; PEG calibration): M_n = 12 200 g mol^{-1}; M_w = 13 400 g mol^{-1}; PDI = 1.02.

Micelle Preparation of ABA Triblock Assemblies 5a−d. The ABA triblock assemblies **5a−d** were dissolved in DMF (2 g/L). In a next step, a water volume equal to half-the DMF volume was added under stirring by steps of 50 μL, followed by the addition of the same water volume in one shot. Afterward the solution was dialyzed against water to remove the DMF. The final concentration was about 0.6 g/L. The solutions have been filtered through 1 μm filters before the DLS measurements. For cryo-TEM measurements the solutions have been prepared in the same fashion without further filtration.

Results and Discussion

This contribution reports on the preparation, characterization, and micellization of the metallo-supramolecular coil−rod−coil **5a−d** that are reminiscent of **ABA** triblock copolymers (Figure 1 and Scheme 1). In the following, we will shortly identify the discussed structures **5a−d** as **ABA** triblock assemblies. These **ABA** triblock assemblies **5a−d** consist of a hydrophilic random coil block **A** based on terpyridine modified poly(ethylene glycol) **1** and a hydrophobic segment **B** based on various rigid-rod-like bis(terpyridine) ligands **4a−d**. Since both mentioned macromonomers are carrying chelating units, their metal complexation could be achieved via a stepwise Ru(II) terpyridine complexation leading to the formation of well-defined **ABA** triblock assemblies architectures.

The complexation approach via $Ru(DMSO)_4Cl_2$ was adopted as an alternative and more advantageous method to coordinate Ru(II) to the terpyridine moiety of both chelating blocks (**A** and **B**) in comparison to the $RuCl_3$ route which normally requires the presence of a reductive agent and sometimes more harsh reaction conditions.[5,18,46] To the best of our knowledge, the combination of hexafluoroantimonate ($AgSbF_6$) with Ru(II) monocomplex monoterpyridine-functionalized polymer **2** has not been described previously, and this combination might overcome some of the difficulties met in the $RuCl_3$ procedure. On the other hand, the presence of a bulky counterion such as SbF_6^- from the beginning of the reaction makes the complexation step to be straightforward since there is no need of

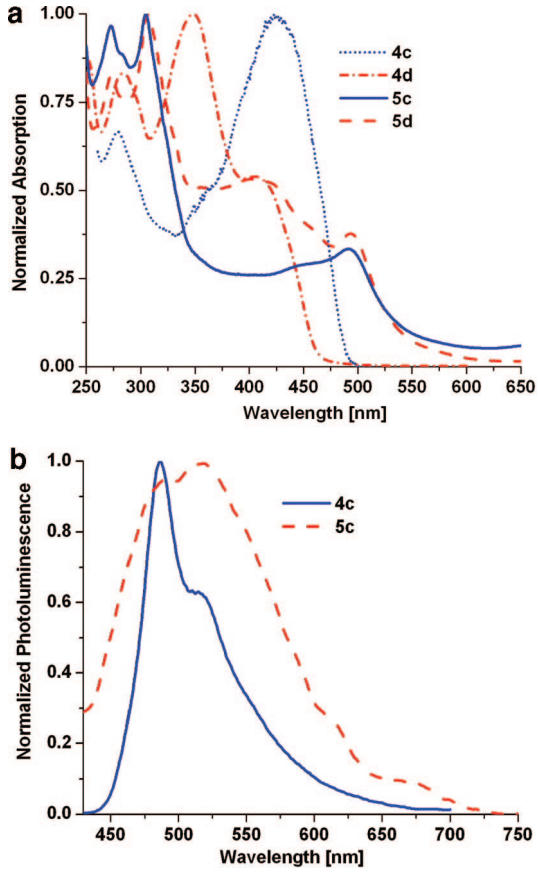

Figure 4. (a) Comparison of the normalized absorption spectra of bis(terpyridine) ligands **4c,d** and their corresponding **ABA** triblock assemblies **5c,d**. All spectra were recorded at 10^{-5} M in $CHCl_3$ or CH_3CN, respectively. (b) Comparison of the normalized emission spectra of bis(terpyridine) ligand **4c** and the corresponding Ru(II) **ABA** triblock assemblies **5c**. All spectra were recorded at 10^{-5} M in $CHCl_3$ or CH_3CN, respectively; excitation at $\lambda_{ex} = 400$ nm.

counterion exchange at the end of the complexation process as it is the case when chloride anions are used (exchange from Cl^- to PF_6^- or other bulky ions). The chemical scheme starts from monoterpyridine−poly(ethylene glycol) **1** (see Supporting Information) that was used to synthesize the monocomplex macroligand **2** (Scheme 1) which represents the key building block[47] in the preparation of the **ABA** triblock assemblies **5a**−**d**. By treating monoterpyridine−poly(ethylene glycol) **1** with $Ru(DMSO)_4Cl_2$ in chloroform, followed by overnight reflux conditions, the monocomplex macroligand **2** was synthesized.[48] The crude reaction mixture was purified by preparative size exclusion chromatography (BioBeads SX-1, CH_2Cl_2), followed by precipitation from dichloromethane into diethyl ether yielding a red-brownish powder. The UV−vis spectrum of **2** revealed the characteristic metal-to-ligand charge transfer (MLCT) bands of the monocomplex at 477 nm, proving the successful incorporation of Ru(II) into the monoterpyridine-functionalized polymer **1**. The SEC trace (Figure 2) showed a monomodal distribution for the prepared monocomplex macroligand **2** with a slightly increased molecular weight in comparison to the uncomplexed starting material **1**. The ^{1}H NMR spectrum of **2** revealed a clear shift for the complexed terpyridine protons due to vicinity of the Ru(II)$DMSOCl_2$ group. The 6,6″-terpyridine protons, which were detected at 8.68 ppm in the uncomplexed ligand **1**, were strongly shifted to a lower magnetic field (9.21 ppm) in the monocomplex macroligand **2**, confirming the formation of monocomplex macroligand **2**.[48]

Prior to the synthesis of the **ABA** triblock assemblies based on a Ru(II) connectivity, the symmetric Ru(II) complex **3** based on monoterpyridine end-functionalized poly(ethylene glycol) **1** was prepared and characterized. Taking into account that the metal complexation of telechelic ligands (e.g., **4a**−**d**) can in theory also lead to the formation of defect structures such as **A**−**A** or **A**−**B** (apart from the desired **ABA**), complex **3** represents a model compound for the corresponding **ABA** supramolecular triblock assemblies **5a**−**d**. Comparison of the characteristics of the **ABA** triblock assemblies with the model complex (e.g., ^{1}H NMR signals or SEC curves) represents a very helpful method to evaluate the success of the reactions and the purity of the obtained supramolecular systems.

The model complex **3** was synthesized starting from the monocomplex macroligand **2** which was treated in the first reaction step with $AgSbF_6$ in acetone followed by the addition of monoterpyridine poly(ethylene glycol) **1**. Further purification of the crude product yielded the pure bis-complex **3**, which was characterized by ^{1}H NMR, SEC, and UV−vis. The ^{1}H NMR spectrum of **3** revealed a characteristic fingerprint for the complexed terpyridine protons: a strong upfield shift of the 6,6″-signal in the bis(terpyridine) complex due to the different chemical environment of the 6,6″-protons, compared to the free ligand **1** and the monocomplex macroligand **2**. In addition, the UV−vis spectrum showed a bathochromic shift from 477 to 490 nm of the metal-to-ligand charge-transfer (MLCT) transitions. The SEC analysis of **3** (Figure 2) displayed, as expected, an increased molecular weight in comparison to the starting materials **1** and **2**.

To synthesize the **ABA** triblock assemblies **5a**−**d**, the general synthetic strategy described in Scheme 1 was followed. In the first step macroligand monocomplex **2** was treated with $AgSbF_6$, resulting in dehalogenation and coordination of acetone ligands to the metal sphere to generate a more reactive ruthenium(II) synthon. In the second step, after the removal of the formed AgCl, the intermediate was reacted with the conjugated ditopic terpyridine ligands **4a**−**d**. The obtained crude products were purified by preparative size exclusion chromatography (Bio-Beads SX-1, CH_2Cl_2) where the byproduct could successfully be removed. The purified triblock assemblies **5a**−**d** were obtained as red-brownish solids in yields between 25 and 50%. They were characterized by SEC, ^{1}H NMR, UV−vis, emission spectroscopy, and cyclic voltammetry (Table 1).

Characterization of the ABA Triblock Assemblies 5a−**d.** From the results of size exclusion chromatography measurements (SEC, see Figure 2) it is obvious that the purified **ABA** triblock assemblies **5a**−**d** have higher molecular weights than the starting material **1**, the monocomplex macroligand **2**, and the model complex **3**, while a monomodal molecular weight distribution is retained. The hydrodynamic volumes of the synthesized **ABA** triblock assemblies seem to be influenced by the different structures of block **B** whereby it should be noted that this correlation is not yet fully understood. For the **ABA** triblock assemblies **5a** and **5b**, SEC analysis revealed a narrow molecular weight distribution while for **5c** and **5d** the molecular weight distributions are more broadened. The results obtained from the SEC with in-line diode array detector of the purified **ABA** triblock assemblies **5a**−**d** (Figure 3) demonstrate the presence and the stability of the supramolecular moieties over the complete molecular weight distribution as indicated by the MLCT band around 500 nm, which is characteristic for the Ru(II) bis(terpyridine) complexes. The ^{1}H NMR spectra for the **ABA** synthesized triblock assemblies **5a**−**d** revealed clear shifts, similar to the model complex, for the complexed terpyridine protons as well as the expected integral ratios proving the successful formation of the desired **ABA** triblock assemblies. The assignments for the aromatic protons were done by two-dimensional ^{1}H−^{1}H correlation spectroscopy (^{1}H−^{1}H COSY). The signals between 4 and 5 ppm could be attributed to the

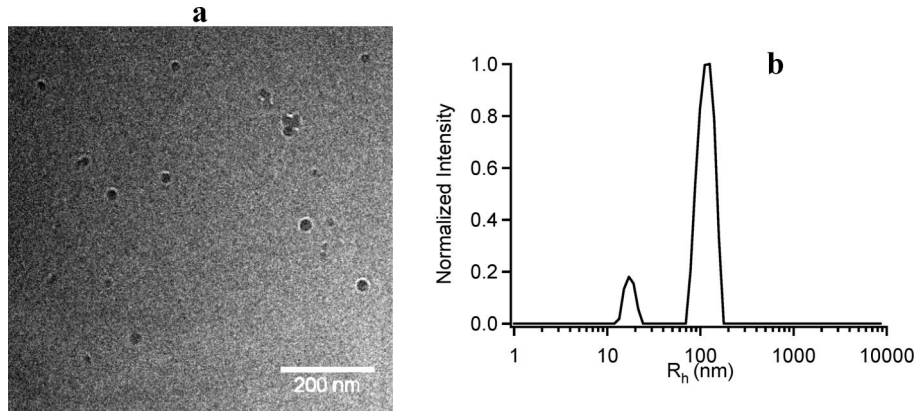

Figure 5. Cryo-TEM (a) and DLS (b) for the micelles obtained from **ABA** triblock assemblies **5a**.

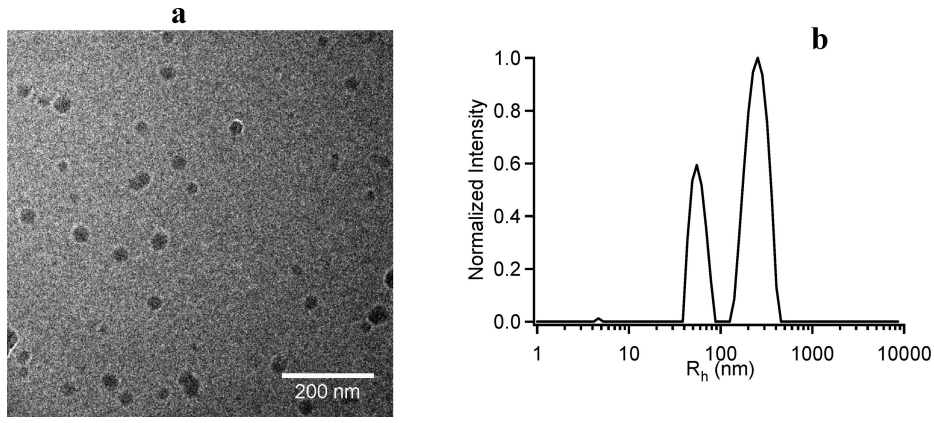

Figure 6. Cryo-TEM (a) and DLS (b) for the micelles obtained from the **ABA** triblock assemblies **5b**.

Table 2. Cryo-TEM and DLS Average Sizes of the Prepared Micelles Containing Ru(II) ABA Triblock Assemblies 5a−d

		DLS R_h [nm]	
ABA triblock assemblies	cryo-TEM R_h [nm]	micelles	aggregates
5a	9.5	19	120
5b	14	47	250
5c	16	42	257
5d	13	25	188

proton signals of the methylene groups next to the terpyridines (α-methylenes) and the strong signal around 3.7 ppm to the other methylene protons of the poly(ethylene glycol) backbone.

Photophysical and Electrochemical Investigations. The photophysical properties of the rigid conjugated ditopic spacers **4a−d** and their corresponding supramolecular triblock copolymers **5a−d** were investigated namely by the absorption maxima, λ_a, the optical band gap energy, E_g^{opt} (estimated from low-energy edge of the absorption spectra), the emission maxima, λ_{em}, and the fluorescence quantum yields, Φ_{fl}. In order to allow a direct comparison between the complexed and uncomplexed studied structures (including the already published ditopic ligands **4a−d**), all results are represented in Table 1.

The absorption spectra of the bis(terpyridine) ligands **4c,d** and the binuclear Ru(II) **ABA** complexes **5c,d** are depicted in Figure 4a. All absorption spectra of the uncomplexed ligands **4a−d** in chloroform show a sharp band at around 280 nm corresponding to the terpyridine moieties. The very intense broad band in the visible region (350−450 nm) can be attributed to the $\pi-\pi^*$ electronic transitions of the backbone conjugated linkages between the terminal terpyridine units. As expected, the strongest bathochromic shift was observed for the thiophene-containing derivative **4c**.[22] In the UV−vis spectra of the Ru(II) **ABA** complexes **5a−d** (recorded in acetonitrile) a set of absorption bands below $\lambda = 300$ nm is present and assigned to the $\pi \rightarrow \pi^*$ transitions of the complexed terpyridines. In comparison to **4a−d**, the intensity of the spacer-based $\pi \rightarrow \pi^*$ transitions (around 400 nm) is decreased significantly. The metal-to-ligand charge transfer (MLCT) band at around 495 nm is characteristic for octahedral Ru(II) bis(terpyridine) complexes.[3]

The MLCT absorption of **5c,d** is shifted to slightly lower wavelength. Upon complexation with Ru(II), the highest occupied molecular orbital (HOMO) of the bis(terpyridine) ligands **4a−d** is lowered in these cases because of the relatively electron-poor nature of the spacer units. The difference Δ_0 to the energy level of the lowest unoccupied molecular orbital (LUMO) is increased, resulting in a shift of the MLCT band toward lower wavelengths.[49] Because of the electronic nature (increased electron density of the spacer), this effect is least pronounced for the thiophene containing materials **4c** and **5c**.

While luminescence studies at low temperature and in the solid state will be the focus of future work, we investigated the emission properties of the Ru(II) **ABA** triblock assemblies **5a−d** at room temperature. The selected photoluminescence spectra of **4c** and **5c** are depicted in Figure 4b. The emission spectra were recorded after excitation at $\lambda_{ex} = 400$ nm. We previously reported on the emission of rigid-rod ditopic terpyridyl ligands **4a−d** covering the blue range (425−500 nm) with high quantum yields up to 85%.[22] A broadening of the emission of the supramolecular materials **5a−d**, with their maxima shifted to 470−550 nm in comparison to **4a−d**, was observed. However, the quantum yield Φ_{fl} of the complexes **5a−d** is decreased dramatically by a factor of 8−10. This led us to the conclusion that the major part of the excitons formed upon excitation of the ligand is transferred to the complex.[49] Since the conjugated systems are emitting in the range where the complex absorbs,

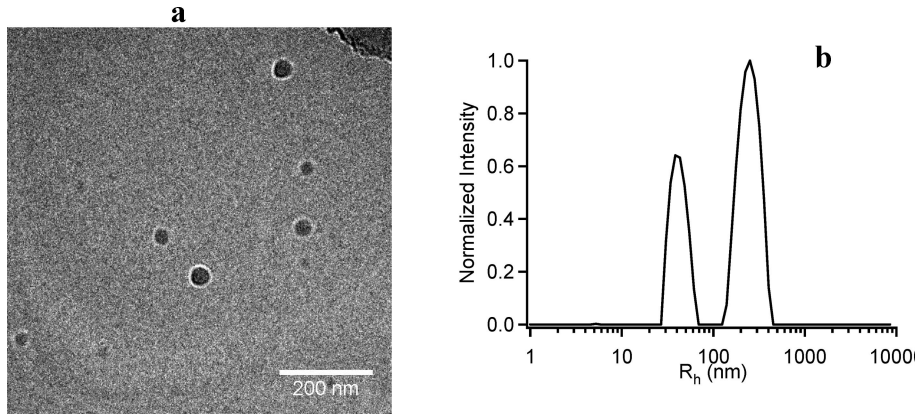

Figure 7. Cryo-TEM (a) and DLS (b) for the micelles obtained from **ABA** triblock assemblies **5c**.

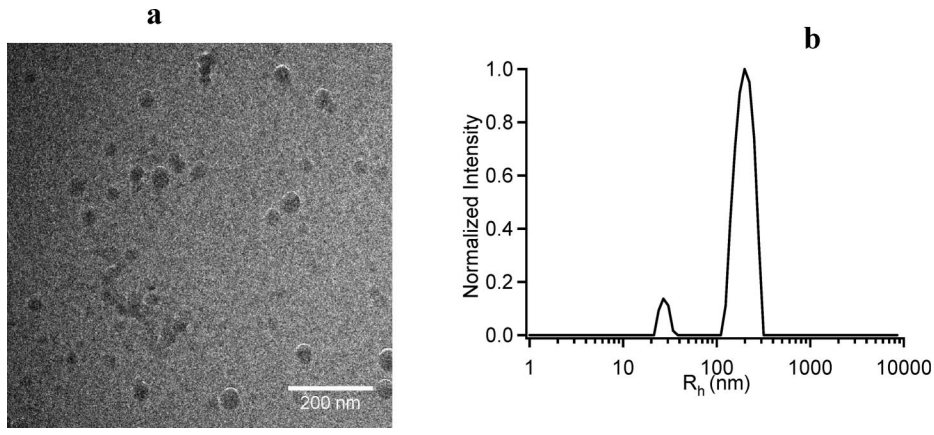

Figure 8. Cryo-TEM (a) and DLS (b) for the micelles obtained from **ABA** triblock assemblies **5d**.

this energy transfer may be assigned to be of the Förster type.[50] In full agreement with the literature,[51] only very weak emission of the complexes at room temperature (around 650 nm) was observed. Thus, the transfer of energy from the π-conjugated spacer to the complex causes a strong quenching of luminescence. These photophysical properties of the supramolecular **ABA** triblock assemblies **5a**−**d** prove once again the formation of the Ru(II)tpy_2 connectivity between the two utilized terpyridine blocks (**A** and **B**).

The redox behavior of the synthesized Ru(II) **ABA** triblock assemblies **5a**−**d** and model complex **3** has been studied in dichloromethane by cyclic voltammetry (CV), and the results are summarized in Table 1. The oxidation potentials are in agreement with the literature data for Ru(II) bis(terpyridine) complexes[52] showing that the electrochemical properties are mainly ruled by the metal complex and not by the ligand itself. For the **ABA** triblock assemblies **5a**−**d** the Ru(II/III) wave is enlarged in comparison to the model complex **3** due to the fact that the two Ru(II) centers are oxidized approximately at the same potential. The presence of a single broadened wave supports the idea that these metal centers are not in electronic interaction but are influenced by the chain length of the spacer.

Micellization of the ABA Triblock Assemblies. The synthesized amphiphilic Ru(II) **ABA** triblock assemblies **5a**−**d** were not directly soluble in water. Therefore, the **ABA** triblock assemblies were first dissolved in *N,N*-dimethylformamide (DMF), which is a good solvent for all blocks, followed by the slow addition of water to trigger micellization. Upon addition of water to the DMF solution of the triblock assemblies **5a**−**d**, aggregation of the block copolymers is expected to induce the formation of self-assembled structures with the hydrophobic segment **B** in the core of the micelles and the hydrophilic block **A** as stabilizing corona. Subsequently, the organic solvent was removed by dialysis,[53,54] leading to the formation of kinetically frozen aggregates, which mirror the self-assembly state in the initial DMF/water mixture.[55] The final micelles in pure water after dialysis are thus locked structures with a rigid core in which no unimer−micelle equilibrium is observed. Such systems have been previously referred to as "kinetically frozen micelles".[55] From previous studies performed on "metallo-supramolecular micelles" based on Ru(II) terpyridine connectivity, we assume that the bis(2,2′:6′,2″-terpyridine)Ru(II) complexes will be located at the core−corona interface.[42] Taking into account that Ru(II) ions are characterized by a high binding strength toward terpyridine ligands and that the bis(terpyridine)Ru(II) complexes are known to be inert complexes, we can expect that the amphiphilic **ABA** triblock assemblies will stay intact during the micellization studies.

Cryogenic transmission electron microscopy (cryo-TEM) and dynamic light scattering (DLS) were utilized to characterize the micelles formed by the self-assembly of the **ABA** triblock assemblies **5a**−**d**. The DLS results (Figures 5b−8b) revealed the presence of two different populations of objects. This observation is in agreement with previous studies performed on metallo-supramolecular micelles with a PEG corona, which have shown that such micelles have a rather strong tendency to form large aggregates.[54,56] Moreover, a previous investigation on metallo-supramolecular micelles combining DLS and cryo-TEM results revealed that the first population observed in the CONTIN histogram could not be attributed to only individual micelles but rather corresponded to individual micelles plus small clusters of micelles (i.e., dimers, trimers, tetramers, etc., of individual micelles).[56] This situation results from a limitation of the CONTIN analysis that is not able to resolve individual

micelles from small clusters. On the other hand, the second population could be attributed to large aggregates of micelles.[56] The same situation prevails in the present study, and it is therefore not possible to correlate the DLS results (Figures 5b−8b) to results obtained by imaging techniques (e.g., cryo-TEM). Cryo-TEM shows that spherical micelles are obtained for all triblock assemblies **5a**−**d** (Figures 5a−8a). For the reason discussed above, the size of the micellar core (R), measured from the images, does not correlate well with the R_h obtained by DLS for the first population (Table 2). Although their **B** middle segments are very short, the **ABA** triblock assemblies investigated in this study can be seen as coil−rod−coil copolymers. Compared to block copolymers only composed of coiled blocks, the self-assembly of coil−rod−coil block copolymers is no longer solely determined by phase separation between the blocks but can be also affected by other processes, e.g., the aggregation of the rodlike segments into (liquid) crystalline domains.[57] Such a phenomenon is able to lead to micelles with peculiar morphologies, including vesicles, tubules, etc.[57] The method used for micelle preparation obviously impedes any aggregation of the rigid **B** segments in (liquid) crystalline domains since only spherical micelles have been formed in agreement with the composition of the investigated **ABA** triblock assemblies that contain a minor volume fraction of unsoluble **B** segments.

Conclusion

We discussed the synthesis and characterization of the supramolecular assemblies **5a**−**d** using as hydrophilic block monoterpyridine end-functionalized poly(ethylene glycol) **1** and as hydrophobic segment different rigid-rod conjugated ditopic terpyridyl ligands **4a**−**d**. The Ru(II) complexation of the utilized chelating ligands followed for the first time a different route in comparison to what has been described previously. The photophysical and electrochemical properties of the novel synthesized materials were studied in solution and compared to the uncomplexed rigid-rod conjugated ditopic ligands **4a**−**d**. The results revealed that there is a strong influence of the metal complex on the photophysical properties of the designed structures **5a**−**d**. Furthermore, due to their amphiphilic properties, the synthesized Ru(II) supramolecular **ABA** triblock assemblies **5a**−**d** self-assembled in aqueous solution. Spherical micelles that are clustering into larger structures were obtained for all **ABA** triblock assemblies as observed by cryo-TEM and DLS. Future work will include detailed morphology studies in different solvents of the **ABA** triblock assemblies bearing different counterions.

Acknowledgment. This study was supported by the Dutch Polymer Institute (DPI project #447) and the Nederlandse Organisatie voor Wetenschappelijk Onderzoek (NWO, open competition and VICI award for U.S.S.). Dr. Eckhard Birckner (Institute of Physical Chemistry, Friedrich-Schiller-University Jena, Germany) is acknowledged for performing the emission measurements. CAF is Research Associate of the FRS-FNRS. J.F.G. and C.A.F. thank the ESF STIPOMAT Programme and the "Politique Scientifique Fédérale" for financial support in the frame of the "Interuniversity Attraction Poles Programme (PAI VI/27): Functional Supramolecular Systems". TEM imaging was carried out with the support of the cryo-TEM research unit, Eindhoven University of Technology.

Supporting Information Available: Experimental details. This material is available free of charge via the Internet at http://pubs.acs.org.

References and Notes

(1) Lehn, J.-M. *Chem. Soc. Rev.* **2007**, *36*, 151–160.
(2) Lehn, J.-M. *Supramolecular Chemistry - Concepts and Chemistry*; VCH: Weinheim, Germany, 1995.
(3) Newkome, G. R.; He, E.; Moorefield, C. N. *Chem. Rev.* **1999**, *99*, 1689–1746.
(4) Schubert, U. S.; Hofmeier, H.; Newkome, G. R. *Modern Terpyridine Chemistry*; Wiley-VCH: Weinheim, 2006.
(5) Lohmeijer, B. G. G.; Schubert, U. S. *Macromol. Chem. Phys.* **2003**, *204*, 1072–1078.
(6) Gohy, J.-F.; Lohmeijer, B. G. G.; Schubert, U. S. *Macromol. Rapid Commun.* **2002**, *23*, 555–560.
(7) Hofmeier, H.; Hoogenboom, R.; Wouters, M. E. L.; Schubert, U. S. *J. Am. Chem. Soc.* **2005**, *127*, 2913–2921.
(8) Eisenbach, C. D.; Schubert, U. S. *Macromolecules* **1993**, *26*, 7372–7374.
(9) Schmatloch, S.; van den Berg, A.; Alexeev, A. S.; Hofmeier, H.; Schubert, U. S. *Macromolecules* **2003**, *36*, 9943–9949.
(10) Kimura, M.; Sano, M.; Muto, T.; Hanabusa, K.; Shirai, H. *Macromolecules* **1999**, *32*, 7951–7953.
(11) Bernhard, S.; Takada, K.; Díaz, D. J.; Abruña, H. D.; Mürner, H. *J. Am. Chem. Soc.* **2001**, *123*, 10265–10271.
(12) Storrier, G. D.; Colbran, S. B.; Craig, D. C. *J. Chem. Soc., Dalton Trans.* **1997**, 3011–3028.
(13) Ng, W. Y.; Gong, X.; Chan, W. K. *Chem. Mater.* **1999**, *11*, 1165–1170.
(14) Schubert, U. S.; Eschbaumer, C.; Andres, P.; Hofmeier, H.; Weidl, C. H.; Herdtweck, E.; Dulkeith, E.; Morteani, A.; Hecker, N. E.; Feldmann, J. *Synth. Met.* **2001**, *121*, 1249–1252.
(15) Heller, M.; Schubert, U. S. *Eur. J. Org. Chem.* **2003**, 947–961.
(16) Heller, M.; Schubert, U. S. *J. Org. Chem.* **2002**, *67*, 8269–8272.
(17) Newkome, G. R.; Patri, A. K.; Holder, E.; Schubert, U. S. *Eur. J. Org. Chem.* **2004**, 235–254.
(18) Lohmeijer, B. G. G.; Schubert, U. S. *Angew. Chem., Int. Ed.* **2002**, *41*, 3825–3829.
(19) Barigeletti, F.; Flamigni, L.; Balzani, V.; Collin, J.-P.; Sauvage, J.-P.; Sour, A.; Constable, E. C.; Cargill Thompson, A. M. W. *J. Am. Chem. Soc.* **1994**, *116*, 7692–7699.
(20) Berhard, S.; Goldsmith, J. I.; Takada, K.; Abruña, H. D. *Inorg. Chem.* **2003**, *42*, 4389–4393.
(21) Barigeletti, F.; Flamigni, L.; Calogero, G.; Hammarström, L.; Sauvage, J.-P.; Collin, J.-P. *Chem. Commun.* **1998**, 2333–2334.
(22) Winter, A.; Egbe, D. A. M.; Schubert, U. S. *Org. Lett.* **2007**, *9*, 2345–2348.
(23) Constable, E. C.; Cargill Thompson, A. M. W. *Dalton Trans.* **1992**, 3467–3475.
(24) Newkome, G. R.; He, E. *J. Mater. Chem.* **1997**, *7*, 1237–1244.
(25) Newkome, G. R.; Cho, T. J.; Moorefild, C. N.; Mohapatra, P. P.; Godinez, L. A. *Chem.—Eur. J.* **2004**, *10*, 1493–1500.
(26) Schmittel, M.; Ammon, H. *Chem. Commun.* **1995**, 687–688.
(27) Indelli, M. T.; Bignozzi, C. A.; Scandola, F.; Collin, J.-P. *Inorg. Chem.* **1998**, *37*, 6084–6089.
(28) Khatyr, A.; Ziessel, R. *Tetrahedron Lett.* **1999**, *40*, 5515–5518.
(29) Ziessel, R. *Synthesis* **1999**, *11*, 1839–1865.
(30) Winter, A.; Hunmel, J.; Risch, N. *J. Org. Chem.* **2006**, *71*, 4862–4871.
(31) Schmatloch, S.; Schubert, U. S. *Macromol. Rapid Commun.* **2002**, *23*, 957–961.
(32) Heller, M.; Schubert, U. S. *Macromol. Rapid Commun.* **2001**, *22*, 1362–1367.
(33) Hofmeier, H.; Schubert, U. S. *Macromol. Chem. Phys.* **2003**, *204*, 1391–1397.
(34) Gohy, J.-F.; Lohmeijer, B. G. G.; Schubert, U. S. *Chem.—Eur. J.* **2003**, *9*, 3472–3479.
(35) Constable, E. C. *Adv. Inorg. Chem. Radiochem.* **1986**, *30*, 69–121.
(36) Storrier, G. D.; Colbran, S. B.; Craig, D. C. *J. Chem. Soc., Dalton Trans.* **1997**, 3011–3028.
(37) Schütte, M.; Kurth, D. G.; Linford, M. R.; Cölfen, H.; Möhwald, H. *Angew. Chem., Int. Ed.* **1998**, *37*, 2891–2893.
(38) Khatyr, A.; Ziessel, R. *J. Org. Chem.* **2000**, *65*, 3126–3134.
(39) Meier, M. A. R.; Wouters, D.; Ott, C.; Guillet, P.; Fustin, C.-A.; Gohy, J.-F.; Schubert, U. S. *Macromolecules* **2006**, *39*, 1569–1576.
(40) Kelch, S.; Rehahn, M. *Macromolecules* **1999**, *32*, 5818–5828.
(41) Guillet, P.; Fustin, C.-A.; Lohmeijer, B. G. G.; Schubert, U. S.; Gohy, J.-F. *Macromolecules* **2006**, *39*, 5484–5488.
(42) Gohy, J.-F.; Lohmeijer, B. G. G.; Schubert, U. S. *Chem.—Eur. J.* **2003**, *9*, 3472–3479.
(43) Fustin, C.-A.; Guillet, P.; Schubert, U. S.; Gohy, J.-F. *Adv. Mater.* **2007**, *19*, 1665–1673.
(44) Fustin, C.-A.; Lohmeijer, B. G. G.; Duwez, A.-S.; Jonas, A. M.; Schubert, U. S.; Gohy, J.-F. *Adv. Mater.* **2005**, *17*, 1162–1165.

(45) Evans, I. P.; Spencer, A.; Wikinson, G. *J. Chem. Soc., Dalton Trans.* **1973**, 204–209.
(46) Aamer, K.; Tew, A. G. N. *Macromolecules* **2007**, *40*, 2737–2744.
(47) Grosshenny, V.; Ziessel, R. *J. Organomet. Chem.* **1993**, *453*, C19−C22.
(48) Ziessel, R.; Grosshenny, V.; Hissler, M.; Stroh, C. *Inorg. Chem.* **2004**, *43*, 4262–4271.
(49) Duprez, V.; Biancardo, M.; Spanggaard, H.; Krebs, F. C. *Macromolecules* **2005**, *38*, 10436–10448.
(50) Lakowicz, J. R. *Principles of Fluorescence Spectroscopy*, 2nd ed.; Plenum Publishers: New York, 2002.
(51) Collin, J.-P.; Harriman, A.; Heitz, V.; Odobel, F.; Sauvage, J.-P. *J. Am. Chem. Soc.* **1994**, *116*, 5679–5690.
(52) Juris, A.; Balzani, V.; Barigelletti, F.; Campagna, S.; Belser, P.; von Zelewsky, A. *Coord. Chem. Rev.* **1988**, *84*, 85–277.
(53) Guillet, P.; Fustin, C.-A.; Lohmeijer, B. G. G.; Schubert, U. S.; Gohy, J.-F. *Macromolecules* **2006**, *39*, 5484–5488.
(54) Gohy, J.-F.; Lohmeijer, B. G. G.; Schubert, U. S. *Macromolecules* **2002**, *35*, 4560–4563.
(55) Zhang, L.; Eisenberg, A. *Science* **1995**, *268*, 1728–1731.
(56) Regev, O.; Gohy, J.-F.; Lohmeijer, B. G. G.; Varshney, S. K.; Hubert, D. H. W.; Schubert, U. S. *Colloid Polym. Sci.* **2004**, *282*, 407–411.
(57) Klok, H.-A.; Lecommandoux, S. *Adv. Mater.* **2001**, *13*, 1217–1229.
(58) Demas, C.; Crosby, G. A. *J. Phys. Chem.* **1971**, *75*, 991–1024.

MA801217V